

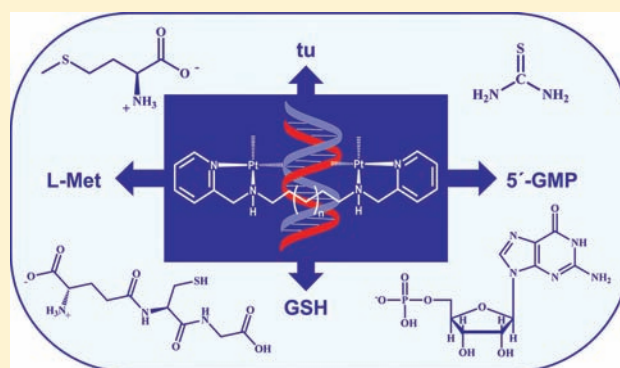
# Reactivity of a Cytostatic Active *N,N*-Donor-Containing Dinuclear Pt(II) Complex with Biologically Relevant Nucleophiles

Stephanie Hochreuther and Rudi van Eldik\*

Inorganic Chemistry, Department of Chemistry and Pharmacy, University of Erlangen-Nürnberg, Egerlandstr. 1, 91058 Erlangen, Germany

## Supporting Information

**ABSTRACT:** A dinuclear platinum(II) complex that was recently investigated in our group was tested for its cytostatic activity and found to be active against HeLa S3 cells. The complex consists of a bidentate *N,N*-donor chelating ligand system in which the two platinum centers are connected by an aliphatic chain of 10 methylene groups. The complex  $[\text{Pt}_2(\text{N}^1, \text{N}^{10}\text{-bis}(2\text{-pyridylmethyl})\text{-}1,10\text{-decanediamine})(\text{OH}_2)_4]^{4+}$  (**10NNpy**) is of further special interest, since only little is known about the substitution behavior of such dinuclear platinum complexes that contain a bidentate coordination sphere. The complex was investigated using different biologically relevant nucleophiles, such as thiourea (tu), *L*-methionine (*L*-Met), glutathione (GSH), and guanine-5'-monophosphate (5'-GMP), at two different pH values (2 and 7.4). The substitution of coordinated water by these nucleophiles was studied under pseudo-first-order conditions as a function of nucleophile concentration, temperature, and pressure, using stopped-flow techniques and UV-vis spectroscopy. The reactivity of **10NNpy** with the selected nucleophiles was found to be  $\text{tu} \gg 5'\text{-GMP} > \text{L-Met} > \text{GSH}$  at pH 2 and  $\text{GSH} > \text{tu} > \text{L-Met}$  at pH 7.4. The results for the dinuclear **10NNpy** complex were compared to those for the corresponding mononuclear reference complex  $[\text{Pt}(\text{aminomethylpyridine})(\text{OH}_2)_2]^{2+}$ , **Pt(amp)**, studied before in our group, by which the effect of the addition of an aliphatic chain, an increase in the overall charge, and a shift in the  $\text{pK}_a$  values of the coordinated water ligands could be investigated. The reactivity order for **Pt(amp)** was found to be  $\text{tu} > \text{GSH} > \text{L-Met}$  at pH 7.4.



## INTRODUCTION

A young woman, Henrietta Lacks, who died in 1951 due to cervical cancer, was the namesake for the first so-called “immortal” human cell line HeLa.<sup>1</sup> Today, the HeLa cell line is used worldwide in biomedical research,<sup>2</sup> and among other things, HeLa cells can be used for cytostatic tests. Since the cytostatic activity of Pt-containing compounds was discovered in 1969,<sup>3</sup> a large number of platinum complexes have been synthesized in an effort to find a treatment for cancer. In a recent study, we synthesized four new dinuclear platinum(II) complexes,<sup>4</sup> which now have been tested with the HeLa S3 cell line for their cytotoxic activity. Thereby, HeLa cells were treated with different concentrations of the Pt(II) complexes and after a specific incubation time, the viability of HeLa cells was determined. One of the studied complexes was able to prevent the aggressive HeLa cells from growing. This cytostatic active complex, namely **10NNpy** (see Figure 1), was chosen in this work for further kinetic investigations.

It is nowadays generally accepted that DNA platination is the ultimate event in the mechanism of action of platinum anti-cancer drugs,<sup>5</sup> but on its route to the DNA target, platinum complexes do also interact with many other biomolecules, especially those containing methionine and cysteine residues.<sup>6</sup> Biomolecules such as methionine and glutathione do interact

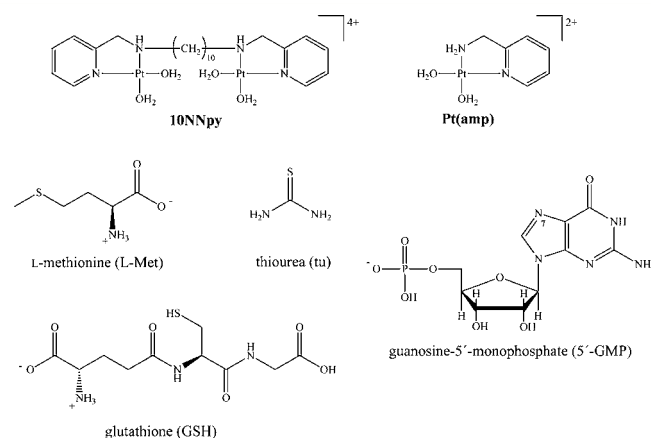


**Figure 1.** Structures of the investigated complexes and nucleophiles, along with the used abbreviations.

with the platinum compound and so compete with nucleobase binding.<sup>7</sup> The question of how platinum can reach the DNA is still not completely solved, but it is hypothesized that at least

Received: October 31, 2011

Published: February 22, 2012

some of the platinum is temporarily bound to S-donor ligands as an intermediate to act like a platinum reservoir,<sup>7,8</sup> before finally interacting and binding to the guanine-N7 atom of DNA.<sup>5</sup> Accordingly, a common hypothesis predicts that Pt–S interactions are kinetically preferred, but the binding of platinum to guanine-N7 is thermodynamically more stable under physiological conditions.

In this study, we focus on two known complexes previously studied in our group, namely a dinuclear bidentate Pt(II) complex with a pyridine unit linked to a secondary amine, where the two metal centers are connected by an aliphatic chain of 10 methylene groups (**10NNpy**),<sup>4</sup> and its mononuclear analogue, **Pt(amp)**,<sup>9</sup> without a bridging element as seen in Figure 1. We used biologically relevant nucleophiles, such as thiourea (tu), L-methionine (L-Met), reduced glutathione (GSH), and guanosine 5'-monophosphate (5'-GMP) for kinetic investigation. Their structures are also included in Figure 1.

Kinetic measurements were performed to study the displacement of coordinated water by several biorelevant molecules in light of the important role that such biomolecules have in terms of understanding the mechanism of anticancer activity.<sup>10</sup> Rate constants for the reaction with glutathione or guanosine-5'-monophosphate are of interest, since these nucleophiles compete with each other within the cell during cisplatin therapy.<sup>5,7,8</sup> Furthermore, the work of Summa et al.,<sup>9</sup> who investigated the kinetic behavior of the **Pt(amp)** complex exclusively at pH 2, was also pursued since we wanted to compare the results of the dinuclear with this mononuclear complex in order to study the differences and similarities in reactivity at pH 2 as well as under physiological conditions.

## EXPERIMENTAL SECTION

**Chemicals.** Deuterated chemicals such as D<sub>2</sub>O, deuterated triflic acid (CF<sub>3</sub>SO<sub>3</sub>D), and NaOD were obtained from Deutero GmbH. The nucleophiles thiourea, L-methionine, glutathione, and guanosine 5'-monophosphate were obtained from Sigma Aldrich. Potassium tetrachloroplatinate(II) was purchased from Strem Chemicals. All other used chemicals were of the highest purity commercially available and were used without further purification. For all preparations of aqueous solutions, ultrapure water was used.

**Preparation of Ligand 1 and Complexes 2 and 3.** The ligand N<sup>1</sup>,N<sup>10</sup>-bis(2-pyridylmethyl)-1,10-decanediamine ligand (**1**) was synthesized following a general literature procedure.<sup>11</sup> The chloro complexes [Pt<sub>2</sub>(N<sup>1</sup>,N<sup>10</sup>-bis(2-pyridylmethyl)-1,10-decanediamine)Cl<sub>4</sub>] (**2**) and [Pt(2-aminomethylpyridine)Cl<sub>2</sub>] (**3**) were synthesized following the general procedure of Hofmann et al.<sup>12</sup> (for more details, see ref 4). During complexation, the NHR<sub>2</sub>-nitrogen donor atom of **10NNpy** becomes a stereogenic center, and several configurations, viz. R<sub>2</sub>R, S<sub>2</sub>S, and S,R are possible. We were not able to isolate the single diastereomers due to rapid H-exchange,<sup>4</sup> and consequently a mixture of all possible configurations was present in solution.

**Preparation of the Complex Solutions.** The desired solutions of the aqua complexes were prepared following a general literature procedure.<sup>12</sup> For kinetic measurements, a complex concentration of 0.2 mM for the **10NNpy** and 0.25 mM for the **Pt(amp)** was chosen. The pH of the complex solutions was adjusted with triflic acid for pH 2 and with Hepes buffer for pH 7.4, respectively.

**Cytostatic Tests.** Cell tests for the recently investigated dinuclear NNpy system and for their corresponding ligands were performed. The cytotoxicity of the chloro complexes was studied using the AlamarBlue assay in the human cervix carcinoma cell line HeLa S3. The AlamarBlue assay is characterized by its linearity and its high sensitivity, while its handling is less error prone in contrast to the MTT assay. Living cells reduce the sodium salt of the dark blue, nonfluorescent dye resazurin (7-hydroxy-3H-phenoxazin-3-one-10-oxide) to the pink, highly fluorescent resorufin (7-hydroxy-3H-phenoxazin-3-one). In the

commonly used MTT assay, the formed formazan is insoluble in the cell-culture medium and needs DMSO as an additional solubilizer. The handling of the AlamarBlue assay is thus much simpler; readout by fluorescence detection is directly achieved without further steps.<sup>13</sup> Cells were cultivated at 37 °C and in 5% CO<sub>2</sub> atmosphere in a DMEM medium (Gibco) with 10% FCS (Biochrome AG) and 1% Pen/Strep (GIBCO) added. Cells were split twice per week. For the assay, cells were seeded in 96-well plates (4000 cells well<sup>-1</sup>) and allowed to attach for 24 h. Complexes to be tested were dissolved in a suitable amount of DMSO. Different concentrations were prepared by serial dilution with a medium to give final concentrations with a maximum DMSO content of 1%. The cells were then incubated for 48 h with 100 μL of each of the above dilution series. After removal of the medium, AlamarBlue solution (10 μL (BioSource Europe) diluted with 90 μL DMEM medium) was directly added, and the cells were incubated for 90 min. After excitation at 530 nm, fluorescence at 590 nm was measured using a Synergy HT Microplate Reader (Bio-TEK). Cell viability is expressed in percent with respect to a control containing only pure medium and 1% DMSO incubated under identical conditions. All experiments were repeated two times with each experiment done in four replicates. The resulting curves were fitted using Sigma plot 10.0 (Systat Software, Inc. 2006).

**Instrumentation and Measurement.** NMR spectroscopy (Bruker Avance DPX 300) and a Carlo Erba Elemental Analyzer 1106 were used for ligand and chloro complex characterization and chemical analysis, respectively. <sup>195</sup>Pt NMR measurements were performed on a Bruker Avance DRX 400WB with K<sub>2</sub>PtCl<sub>4</sub> (in D<sub>2</sub>O/CF<sub>3</sub>SO<sub>3</sub>D) as a reference (δ = -1620 ppm). A Varian Cary 1G spectrophotometer equipped with a thermostatted cell holder was used to record UV-vis spectra for the determination of the pK<sub>a</sub> values of the aqua complexes. Kinetic measurements on fast reactions were performed on an Applied Photophysics SX 18MV stopped-flow instrument, and for the study of slow reactions a Shimadzu UV-2010PC spectrophotometer with a thermo-electrically controlled cell holder was used. Experiments at elevated pressure were performed on a laboratory-made high-pressure stopped-flow instrument for fast reactions,<sup>14</sup> and for slow reactions, they were done on a Shimadzu UV-2101-PC spectrophotometer equipped with a laboratory-made high-pressure cell.<sup>15</sup> To follow reactions at elevated pressures and wavelengths below 300 nm, the HPSF56 high pressure stopped-flow from HighTech was used. The temperature of the instruments was controlled throughout all kinetic experiments to an accuracy of ±0.1 °C.

All UV-vis kinetic experiments were performed under pseudo-first-order conditions with respect to the coordinated water ligands. The values of the reported pseudo-first-order rate constants are the average of at least four kinetic measurements. The pH of 2 was adjusted using 0.01 M triflic acid, whereas the pH of 7.4 was obtained using 0.1 M Hepes buffer and adjusting the pH with drops of concentrated triflic acid. No chloride was added because the dinuclear complexes slowly precipitate in the presence of chloride due to the formation of the insoluble tetrachloro complex.

**Mass Spectrometric Measurements.** To gain more information on the nature of the final products of the reactions with several nucleophiles at different pH values, mass spectrometric measurements were performed. These measurements were performed on a UHR-TOF Bruker Daltonik (Bremen, Germany) maXis, an ESI-TOF mass spectrometer capable of a resolution of at least 40 000 fwhm used by the group of Prof. Ivana Ivanović-Burmazović at the University of Erlangen—Nürnberg. Detection was in the positive-ion mode, and the source voltage was 3.4 kV. The flow rate was 500 μL h<sup>-1</sup>. The drying gas (N<sub>2</sub>) to aid solvent removal was kept at 180 °C. The instrument was calibrated prior to every experiment via direct infusion of the Agilent ESI-TOF low concentration tuning mixture, which provided an m/z range of singly charged peaks up to 2700 Da in both ion modes. A big advantage using this technique is that it only requires low concentrations of the products. For the measurements at pH 2, solutions of 0.05 mM **10NNpy** complex and 0.5 mM of the corresponding nucleophile, both dissolved in 0.01 M triflic acid, were used. Mass spectra were recorded with the solutions before mixing the

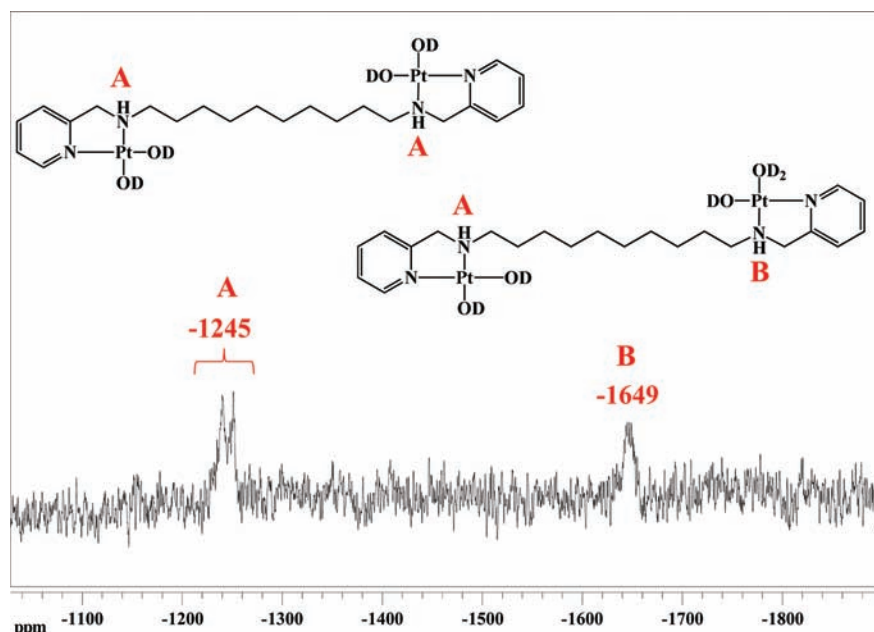


Figure 2.  $^{195}\text{Pt}$  NMR spectrum of the dinuclear **10NNpy** complex at pH 7.4.

complex with the nucleophiles, 24 h after mixing, and finally after 14 days reaction time. The generated peaks were identified and the isotopic pattern simulated.

## RESULTS AND DISCUSSION

**Characterization of Complex Species in Solution at Different pH's.** The tetraaqua complex **10NNpy** exhibits one major peak at  $m/z = 389$  and more, smaller peaks, from which two are selected, viz. at  $m/z = 927$  and  $m/z = 1059$ . The major peak represents **10NNpy** with the contribution  $(\text{C}_{22}\text{H}_{34}\text{N}_4\text{Pt}_2)(\text{OH})_2$ , and the two smaller ones represent  $(\text{C}_{22}\text{H}_{34}\text{N}_4\text{Pt}_2)(\text{CF}_3\text{SO}_3)(\text{OH})_2$  and  $(\text{C}_{22}\text{H}_{34}\text{N}_4\text{Pt}_2)(\text{CF}_3\text{SO}_3)_2(\text{OH})$ , respectively. The major species are 2-fold positively charged, whereas the two less intensive species are both 1-fold positively charged. The isotopic pattern as well as the complete recorded mass spectra are reported in Figures S1–S3 (Supporting Information). The mass spectra of the pure **10NNpy** complex at pH 2 shows only evidence for the dinuclear system; i.e., no dimers or polymers were observed. Such species would exhibit a different isotopic pattern and would therefore have been detected. Besides the complex peaks, a few single peaks could be found that belong to organic moieties and are probably generated during the evaporation process (180 °C).

Usually, OH-bridged dimerization of mononuclear Pt(II) complexes is not considered to be a problem because of the low concentrations in biological medium. However, dinuclear complexes are able to form intramolecular OH-bridged species. In the case of mononuclear complexes, e.g., cisplatin, the hydrolysis and oligomerization processes are well-studied.<sup>16</sup> It was found that after hydrolysis the generated aqua species undergo oligomerization at a pH greater than the  $\text{p}K_a$  of the aqua complex. The hydroxo ligand formed upon deprotonation bridges between the two Pt(II) centers and forms dimeric and trimeric species.<sup>17</sup> Besides the biological relevance, the formation of  $\mu\text{-OH}$  bridged dimers is of special interest in this study, since kinetic investigations were carried out at higher pH and intramolecular OH-bridged species may very well exist at pH 7.4. Therefore, the aqua complexes of **10NNpy** and **Pt(amp)** were investigated using  $^1\text{H}$  and  $^{195}\text{Pt}$  NMR measurements at

pH 2 and 7.4 to identify the species present at each pH. For this purpose, the aqua complexes were synthesized as described in the Experimental Section using  $\text{D}_2\text{O}$  instead of  $\text{H}_2\text{O}$ , and the pH was adjusted using deuterated triflic acid ( $\text{CF}_3\text{SO}_3\text{D}$ ) and NaOD. The large  $^{195}\text{Pt}$  chemical shift range could not be sampled in a single experiment due to instrument limitations, and two specific spectral regions were therefore individually scanned (−1000 to −2000 and −2000 to −3000).

As expected, we observed one single peak for both complexes at pH 2, where the diaqua and tetraaqua complexes are exclusively present in solution. The  $^1\text{H}$  and  $^{195}\text{Pt}$  NMR spectra are depicted in Figures S4–S6 and prove the purity of the aqua complexes. Due to the symmetry of the dinuclear **10NNpy** complex, only one peak for both Pt(II) metals is observed. The chemical shifts for both complexes are very similar, viz.  $\delta(\text{10NNpy}) = -1666$  ppm and  $\delta(\text{Pt(amp)}) = -1640$  ppm, which is in good agreement with platinum compounds in the oxidation state +II.<sup>16,18</sup>

At a higher pH of approximately 7.4, more peaks were found for the **10NNpy** complex. This is not surprising since at such a pH more than one species exists in solution. Figure 2 shows the  $^{195}\text{Pt}$  spectrum of the dinuclear **10NNpy** complex. According to the determined  $\text{p}K_a$  values for **10NNpy**, there should be a mixture of mono-aqua-trihydroxo (56%), tetrahydroxo (39%), and diaqua-dihydroxo (5%) species present at pH 7.4 (see structures in Figure 2).<sup>4</sup> The contribution of the diaqua-dihydroxo compound with 5% is quite small and was not observed in the  $^{195}\text{Pt}$  NMR spectrum. Two signals were observed for the dinuclear **10NNpy** complex. We assume that the doublet around −1245 ppm belongs to the Pt(II) metals surrounded by two OD ligands. The splitting of this peak may be due to a mixture of OD and OH ligands on the Pt(II) center. Furthermore, the single peak at −1649 ppm can be ascribed to the Pt(II) metal coordinated by an OD and an  $\text{OD}_2$  ligand. Compared to the aqua species at pH 2, the  $\text{Pt}(\text{OD})(\text{OD}_2)$  signal is shifted about 20 ppm downfield, which is due to the OD ligand within the coordination sphere. The platinum center with two OD ligands,  $\text{Pt}(\text{OD})_2$ , can be found another 400 ppm downfield shifted due to the deshielding of

**Table 1.** Summary of Rate Constants for the Displacement of Coordinated Water by a Range of Nucleophiles at Various pH and Temperature

	<i>T</i> in °C	pH	<i>k</i> <sub>1</sub> or <i>k</i> <sub>3</sub> in M <sup>-1</sup> s <sup>-1</sup>		<i>k</i> <sub>2</sub>	
			Pt(amp)	10NNpy	Pt(amp) <sup>9</sup>	10NNpy
tu	25	2	233 ± 5 <sup>9</sup>	52.2 ± 0.3 <sup>4</sup>	38 ± 1 M <sup>-1</sup> s <sup>-1</sup>	0.35 ± 0.01 <sup>4</sup> M <sup>-1</sup> s <sup>-1</sup>
	37	7.4	1.40 ± 0.02	0.424 ± 0.007		
L-Met	25	2	2.15 ± 0.05 <sup>9</sup>	1.86 ± 0.02	(0.12 ± 0.03) × 10 <sup>-3</sup> s <sup>-1</sup>	(0.13 ± 0.03) × 10 <sup>-3</sup> s <sup>-1</sup>
	37	7.4	0.381 ± 0.002	0.030 ± 0.001		
GSH	25	2	0.406 ± 0.005	0.500 ± 0.006		
	40	2		1.04 ± 0.01		(0.26 ± 0.01) × 10 <sup>-4</sup> s <sup>-1</sup>
	37	7.4	0.71 ± 0.01	1.65 ± 0.02		
5'-GMP	40	2	12.5 ± 0.5 <sup>9</sup>	3.75 ± 0.07	0.97 ± 0.02 M <sup>-1</sup> s <sup>-1</sup>	0.81 ± 0.01 M <sup>-1</sup> s <sup>-1</sup>

the metal center. Finally, we note that **10NNpy** is poorly soluble since it includes a long aliphatic chain. On increasing the pH, the signal splits into two peaks, and the intensity of each peak decreases. Therefore, the signal-to-noise ratio for the <sup>195</sup>Pt spectra is rather poor, but at least the signals are visible. The mononuclear reference complex **Pt(amp)** was investigated as well. Only one signal could be found in the same region at -1245 ppm, which can be ascribed to the Pt(OD)<sub>2</sub> moiety. A signal for the mixed coordination sphere Pt(OD)(OD<sub>2</sub>) was not observed. The <sup>195</sup>Pt spectrum for **Pt(amp)** at pH 7.4 is depicted in Figure S7.

**Kinetic Measurements.** The kinetics of the substitution of coordinated water were investigated spectrophotometrically by following the change in absorbance as a function of time using UV-vis and stopped-flow techniques. The spectral changes that accompany the reaction were studied over the wavelength range 200–400 nm to establish a suitable wavelength at which the substitution reactions could be followed. A summary of the used wavelengths for each nucleophile can be found in Table S1 (Supporting Information). The investigated nucleophiles tu, L-Met, GSH, and 5'-GMP were used because of their different nucleophilicity, steric hindrance, binding properties, and biological relevance. Kinetic investigations were done at pH 2 (0.01 M triflic acid) to obtain more information about the reactivity of each nucleophile with the N,N-complex system. Since polynuclear Pt(II) complexes are used as anticancer agents, there is much interest in investigating and comparing the properties of such systems under physiological conditions. For that reason, measurements at pH 7.4 and 37 °C were also performed. To keep a constant pH of 7.4, a 0.1 M Hepes buffer was used for all measurements (Hepes = 4-(2-hydroxyethyl)-1-piperazineethanesulfonic acid). This buffer was selected because it is sterically more crowded than, e.g., Tris buffer (Tris = tris(hydroxymethyl)aminomethane), and as a consequence Hepes does not coordinate as strongly to the Pt(II) center as, e.g., Tris buffer does.<sup>19</sup> To mimic physiological conditions, it would in principle be necessary to use a specific chloride concentration. Unfortunately, the dinuclear **10NNpy** complex slowly precipitates in the presence of chloride ions due to the low solubility of the corresponding tetrachloro complex. This is not acceptable when using UV-vis spectroscopy to monitor the reaction progress. We, therefore, neglected the influence of chloride and worked under physiological conditions in terms of pH and temperature.

As mentioned before, the substitution reactions were studied under pseudo-first-order conditions with respect to either the Pt(II) complex or the nucleophile concentration to force the reactions to go to completion. Due to the stereogenic nitrogen donor atom of the NHR<sub>2</sub> unit, and the possibility of H-exchange

at this nitrogen atom, there should always be a mixture of diastereomers and enantiomers present in solution. During the kinetic experiments, no evidence was observed for the different reactivity of the different species in solution. We assume that the configuration at the NHR<sub>2</sub> unit does not affect the rate of the substitution reactions, since the hydrogen atom that can switch its position is small and sterically nondemanding. The mononuclear reference complex **Pt(amp)** includes no stereogenic center after complexation due to its NH<sub>2</sub> group.

**Reactions with Thiourea.** Thiourea (tu) is a biphilic nucleophile, since it combines the ligand properties of thioates<sup>20</sup> (π donors) and thioethers<sup>21</sup> (σ donor, π acceptor), and is furthermore an often used nucleophile due to its good solubility, neutral character, and high nucleophilicity. Furthermore, tu is of biological interest because it can act as a so-called protecting agent to reduce nephrotoxicity.<sup>7,10</sup> The replacement of coordinated water was investigated at pH 2 in earlier work for **10NNpy**<sup>4</sup> and **Pt(amp)**<sup>9</sup> as a mononuclear reference complex. The results are summarized here for comparison with data for other nucleophiles and pH values.

Due to the neutral character of thiourea, the charge of the complex does not change during the substitution reaction. Consequently, the dinuclear **10NNpy** complex shows two substitution steps for the displacement of altogether four water molecules, since the two water molecules at each Pt(II) center are equivalent and displaced simultaneously. Plots of *k*<sub>obs1,2</sub> versus thiourea concentration led to a linear dependence with no meaningful intercept for both complexes and both substitution reactions. The results imply that *k*<sub>obs</sub> for the first and second substitution step can be expressed by eqs 1 and 2, where Nu = thiourea, and the results are summarized in Table 1.

$$k_{\text{obs1}} = k_1[\text{Nu}] + k_{-1} \approx k_1[\text{Nu}] \quad (1)$$

$$k_{\text{obs2}} = k_2[\text{Nu}] + k_{-2} \approx k_2[\text{Nu}] \quad (2)$$

The displacement of the first water occurs *trans* to the pyridine unit, which is in contrast to the determined p*K*<sub>a</sub> values, but can be explained by a favored rearrangement of the transition state during the substitution reaction as described previously (for a detailed description of the substitution mechanism of **10NNpy** with thiourea at pH 2, see ref 4).

It is interesting to compare the substitution behavior at pH 2 with the behavior under physiological conditions, since increasing the pH changes the reactivity of the complexes, and different results are therefore expected. At pH 7.4, the **Pt(amp)** complex exists predominantly in its dihydroxo form (85%), and only 15% aqua-hydroxo species are present in solution, as seen in Figure S8. The distribution was calculated on the basis of the recently determined p*K*<sub>a</sub> values for **Pt(amp)** (p*K*<sub>a1</sub> = 4.77,

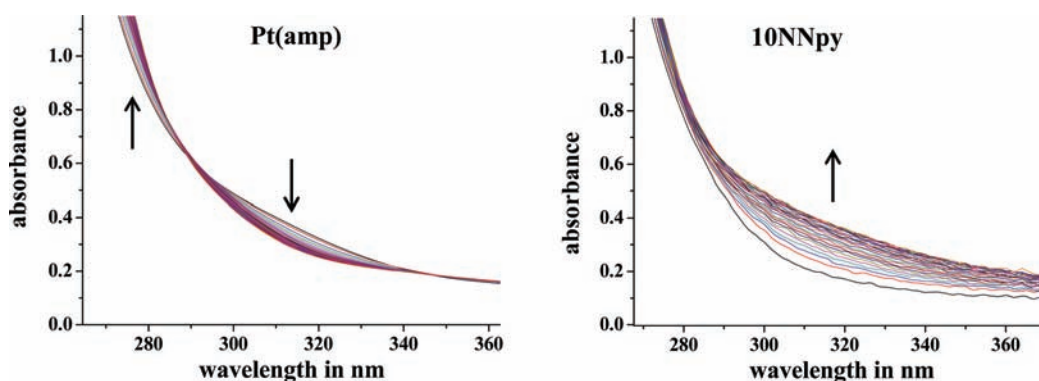
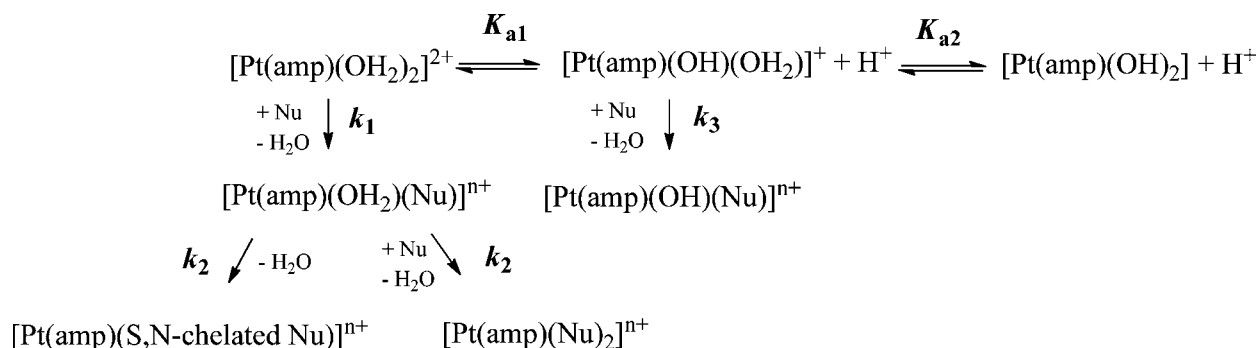


**Figure 3.** UV-vis spectra recorded for the reaction of 0.125 mM **Pt(amp)** (left) and 0.1 mM **10NNpy** (right) each with 5 mM thiourea at pH 7.4 and 25 °C ( $I = 0.1$  M Hepes) for 45 min reaction time. Arrows indicate absorbance increase or decrease.

**Scheme 1. Simplified Substitution Scheme for **Pt(amp)** with Different Nucleophiles (Nu = tu, L-Met, GSH, 5'-GMP, and  $n+$  Depends on the Selected Nucleophile)**



$pK_{a2} = 6.56$ ).<sup>4</sup> Therefore, it is clear that the reactive species have to be the aqua-hydroxo complex, where one remaining water ligand can be substituted. The **10NNpy** complex seems to be more complicated, since it includes four water molecules with four  $pK_a$  values. Figure S9 depicts the distribution diagram as a function of pH with altogether five successively generated species in solution, whereupon no tetraaqua, 5% diaqua-dihydroxo, 56% aqua-trihydroxo, and 39% tetrahydroxo species are present in solution at pH 7.4. Again, this distribution diagram is based on the four  $pK_a$  values determined for **10NNpy**, viz.  $pK_{a1} = 3.77$ ,  $pK_{a2} = 4.20$ ,  $pK_{a3} = 6.45$ , and  $pK_{a4} = 7.56$ .<sup>4</sup> To obtain more information on the substitution behavior of **10NNpy** around the physiological pH, we initially performed pH dependent substitution reactions with thiourea in the pH range 6.0–8.5 (Figure S10 depicts the resulting pH profile). The kinetically determined  $pK_a$  value of  $7.7 \pm 0.9$  is within the error limits close to the value obtained by pH titration. To sum up, we suggest that the active species of **10NNpy** at physiological pH is the monoaqua-trihydroxo species with one labile water molecule left within the coordination sphere, which is stable in solution under the selected conditions, viz. pH 7.4 and  $I = 0.1$  M (Hepes buffer).

Figure 3 shows the absorbance changes that occur during the reaction with thiourea at pH 7.4 for both complexes. The absorbance changes are larger in this case as compared to the changes observed at pH 2.

In general, we found slower reactions at higher pH, which can be accounted for by the formation of hydroxo species that led to a less labile and less electrophilic Pt(II) center. Following deprotonation, the resulting hydroxo ligand was found to be practically inert to substitution, presumably due to a back-bonding

effect of the lone pair electrons on the hydroxo ligand with the  $p_z$  orbital of the metal.<sup>21–23</sup> The **Pt(amp)** complex shows exactly a single reaction step, and the kinetic traces could be fitted perfectly to a single exponential function. As mentioned above, the dihydroxo species is inert to substitution. Therefore, we assume that the only active species at pH 7.4 is the aqua-hydroxo species, where the remaining water molecule is displaced by thiourea. In principle, the coordinated thiourea ligand can affect the  $pK_a$  value of the remaining hydroxo ligand. The decrease in electrophilicity of the Pt(II) center should result in a less acidic  $pK_a$  value. However, in the case of **Pt(amp)**, we observed no further reaction, which indicates that the influence of coordinated thiourea is too weak to significantly change the  $pK_a$  value. Plots of  $k_{\text{obs}3}$  versus thiourea concentration lead to a linear dependence and can be analyzed using eq 3. Scheme 1 summarizes the substitution reaction of **Pt(amp)** with different nucleophiles at pH 7.4. The successive reaction steps described in Scheme 1 were postulated by Summa et al.<sup>9</sup> and were extended for reactions at pH 7.4 in the present study.

$$k_{\text{obs}3} = k_3[\text{Nu}] + k_{-3} \approx k_3[\text{Nu}] \quad (3)$$

In the case of **10NNpy**, two reaction steps were observed, one fast and one remarkably slow reaction. As an example, the kinetic traces for **10NNpy** including the necessary time scales for both reaction steps are depicted in Figure 4 (see also Table S2). We assume that the active species is the monoaqua-trihydroxo species, which is predominantly present in solution (56%). Plots of  $k_{\text{obs}3}$  versus thiourea concentration result in a linear dependence with no intercept, as seen in Figure 5; the results obey eq 3 and are summarized in Table 1. We found a rate constant  $k_3$  of  $0.424 \pm 0.007 \text{ M}^{-1} \text{ s}^{-1}$  for **10NNpy**

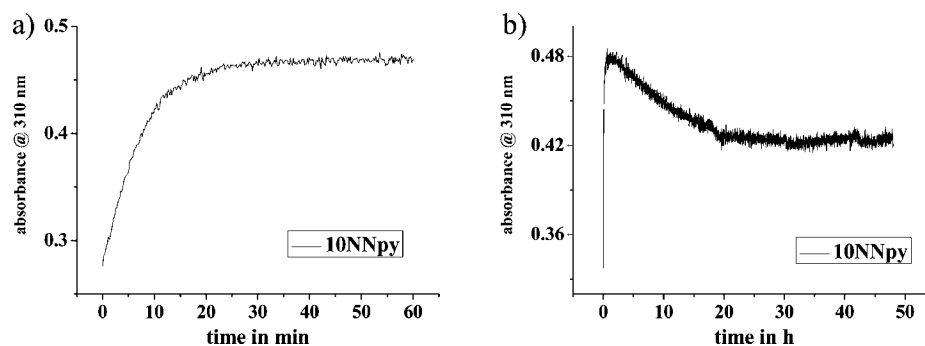


**Figure 4.** Absorbance-time traces for the reaction between **10NNpy** and 5 mM thiourea, (a) on a short time scale for  $k_3$  and (b) on a long time scale for  $k_4$  at pH 7.4.

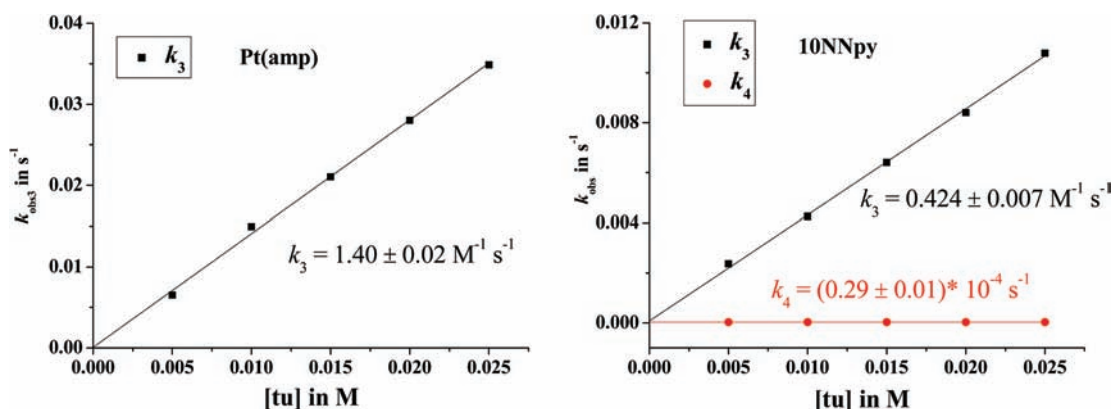
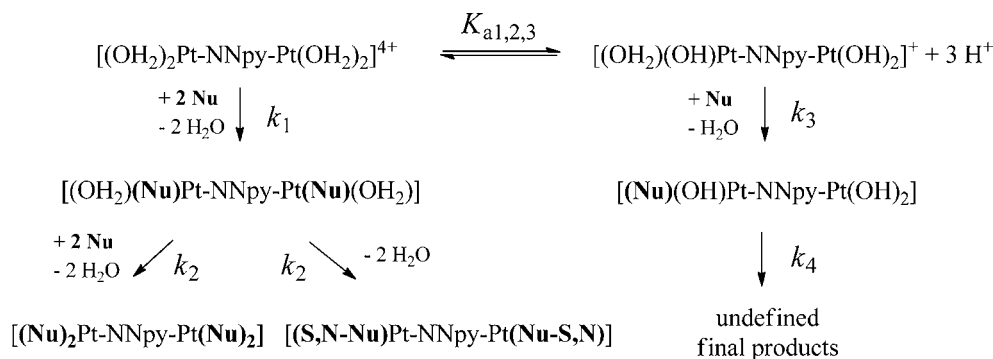


**Figure 5.** Plots of  $k_{\text{obs}3}$  and  $k_{\text{obs}4}$  vs thiourea concentration for the reaction with 0.125 mM **Pt(amp)** and 0.1 mM **10NNpy** at pH 7.4 and 37 °C ( $I = 0.1$  M, Hepes).

**Scheme 2. Proposed Substitution Pathway for the Reaction of 10NNpy with a Nucleophile (Nu) (Charge Omitted for Clarity)**



compared to  $1.40 \pm 0.02 \text{ M}^{-1} \text{ s}^{-1}$  for **Pt(amp)** at 25 °C. We know from a previous study that the first deprotonation steps of **10NNpy** take place *trans* to the pyridine unit.<sup>4</sup> Therefore, the last water ligand is localized *trans* to the secondary amine  $\text{NHR}_2$  at pH 7.4. This assumption was verified using a dinuclear **NNpy** complex with a shorter aliphatic bridge (**4NNpy**). As a result, we found the water displacement to be accelerated ( $k_3 = 1.53 \pm 0.02 \text{ M}^{-1} \text{ s}^{-1}$ ), which can be ascribed to a clear dependence on the bridging element, which consequently proves that the displacement at pH 7.4 takes place *trans* to the  $\text{NHR}_2$  group (Figure S11). A general presentation of the substitution reactions for the dinuclear **10NNpy** complex is presented in Scheme 2.

In contrast, plots of  $k_{\text{obs}4}$  versus thiourea concentration show that the reaction is independent of the nucleophile concentration (Figure 5). On the basis of Scheme 2 and the obtained information on the **Pt(amp)** complex, the second reaction of **10NNpy**

has to involve a reaction step that is independent of the thiourea concentration, or the observed reaction is not the rate-determining step. An acid–dissociation equilibrium, where hydroxo ligands can be protonated due to a change in  $\text{p}K_a$ , can be excluded since it would occur very fast and a subsequent attack of the nucleophile would lead to a concentration dependent process. This very slow reaction can either be due to decomposition of the complex system or formation of oligomers, which both would be independent of nucleophile concentration. We assume that over the long time scale, decomposition processes most probably occur.

**Reactions with L-Met.** The biomolecule L-methionine is a thioether containing an essential amino acid with two acid dissociation constants,  $\text{p}K_{\text{COOH}} = 2.13^{25}$  and  $\text{p}K_{\text{NH}_3^+} = 9.2^{26}$ . On the basis of the  $\text{p}K_a$  values for L-Met, it is clear that at pH 2 the carboxylate group is protonated to an extent of about 50%, resulting in an overall charge of +1. The residual 50% exists in

its zwitterionic form (see Figure 1). Usually, we assume that at pH 2 the reaction takes place between the zwitterion and the positively charged diaqua  $\text{Pt}(\text{amp})$  or tetraaqua  $10\text{NNpy}$  complexes. Even if the positively charged L-Met species would interact with the Pt(II) complex, it is expected to immediately deprotonate due to a significant decrease in the  $\text{p}K_{\text{a}}$  value upon coordination to the metal center. Therefore, the product complex will again be of the same charge as the starting complex. At pH 7.4, the zwitterionic form is predominantly present in solution and interacts with the Pt(II) compound.

Spectral changes of the reaction with L-Met were recorded to establish a suitable wavelength at which the kinetic measurements could be performed. The so-obtained UV-vis spectrum for  $10\text{NNpy}$  is illustrated in Figure S12. L-Met contains different types of donor atoms, but the first nucleophilic attack occurs through the sulfur donor of the thioether group. We found two successive substitution reactions for the  $10\text{NNpy}$  complex, whereupon the first step shows a linear concentration dependence and the second step was found to be independent of the L-Met concentration, typical for a ring-closure reaction that was also observed for the  $\text{Pt}(\text{amp})$  complex. Plots of  $k_{\text{obs}1,2}$  versus L-Met for  $10\text{NNpy}$  are reported in Figure S13 (also Table S3), and the so-obtained rate constants,  $k_1$  and  $k_2$ , are summarized in Table 1. These results are very similar to those reported by Summa et al.<sup>9</sup> and imply that  $k_{\text{obs}1}$  and  $k_{\text{obs}2}$  for  $10\text{NNpy}$  can also be expressed by eqs 1 and 4.

$$k_{\text{obs}2} = k_2 \quad (4)$$

It is noted that the displacement of the first water molecule in the case of  $10\text{NNpy}$  ( $1.86 \pm 0.02 \text{ M}^{-1} \text{ s}^{-1}$ ) is nearly as fast as for the  $\text{Pt}(\text{amp})$  complex<sup>9</sup> ( $2.15 \pm 0.05 \text{ M}^{-1} \text{ s}^{-1}$  at  $25 \text{ }^\circ\text{C}$ ). This behavior is surprising since we found the mononuclear complex to react 4.5 times faster than the dinuclear complex using thiourea as a nucleophile (see Table 1), which is in agreement with the observed  $\text{p}K_{\text{a}}$  values. Furthermore, the metal centers of  $10\text{NNpy}$  are slightly less electrophilic due to the electron donating ability of the aliphatic bridge. We suggest that the entering nucleophile is the crucial factor, because all other factors like pH or electrophilicity of the metal centers are similar in both reactions. However, L-Met as a weak nucleophile is not able to benefit from the different electrophilicities of the Pt(II) centers as thiourea does. A similar behavior was also found in the work of Hofmann et al., who studied the reactions of different mononuclear Pt(II) complexes with a series of nucleophiles.<sup>27</sup>

The final displacement of the remaining water ligands occurs at the same rate, within the experimental error limits, for the mononuclear as for the dinuclear complex with a rate constant  $k_2 = (0.13 \pm 0.03) \times 10^{-3} \text{ s}^{-1}$  (see Table 1), and is independent of nucleophile concentration. Summa et al.<sup>9</sup> were able to prove that the second substitution of  $\text{Pt}(\text{amp})$  with L-Met is due to a chelate formation process, whereupon ring closure was accomplished by the amino group, which leads to a favored six-membered ring. NMR experiments by Appleton et al. confirmed the S,N-chelate to be the only significant product present in solution.<sup>28</sup> However, it should be mentioned that Sadler et al.<sup>29</sup> found that an initial O-binding of L-methionine can also occur as the first substitution step, followed by fast O to S bond conversion. In such a case, O-binding will be the rate-determining step, and a single exponential kinetic trace will be observed if the subsequent O to S bond conversion is fast. Nevertheless, the overall final reaction product will be the S,N-chelated species for  $\text{Pt}(\text{amp})$  as well as for the  $10\text{NNpy}$  complex.

In addition, we note that the substitution behavior of  $10\text{NNpy}$  confirms our assumption of a rather good stability of the din-

uclear system, because the amine linker is not substituted by a second *trans* labilizing L-Met nucleophile as in the case of, e.g., BBR3610, a dinuclear Pt(II) complex studied previously in our group.<sup>30</sup> The decomposition of a polynuclear structure into mononuclear Pt(II) complexes and the aliphatic linker was also reported by Farrell et al. for the reaction with different S-containing nucleophiles.<sup>31,32</sup> By insertion of a chelating ligand, we found an improved complex stability, and degradation of the system occurs very slowly even in the case of stronger nucleophiles like thiourea.<sup>4</sup>

Kinetic investigations with L-Met were also carried out at pH 7.4 and  $37 \text{ }^\circ\text{C}$ . Figure S14 shows the UV-vis spectra for both complexes recorded during the reaction. Compared to the observations at pH 2, the spectral changes are larger. An isosbestic point occurs at 274 nm for  $\text{Pt}(\text{amp})$ , and a rather unclear isosbestic point at 268 nm is observed for  $10\text{NNpy}$ . Substitution of the single coordinated water molecule at pH 7.4 by L-Met leads to a linear concentration dependence with no intercept in both cases, for which the two rate constants differ by a factor of 10, viz.  $k_3 = 0.381 \pm 0.002 \text{ M}^{-1} \text{ s}^{-1}$  for  $\text{Pt}(\text{amp})$  and  $k_3 = 0.030 \pm 0.001 \text{ M}^{-1} \text{ s}^{-1}$  for  $10\text{NNpy}$ . Again, the reactions at pH 7.4 are significantly slower than at pH 2, as seen in Figure 6 and Table 1 (see also Table S4). The sterically more

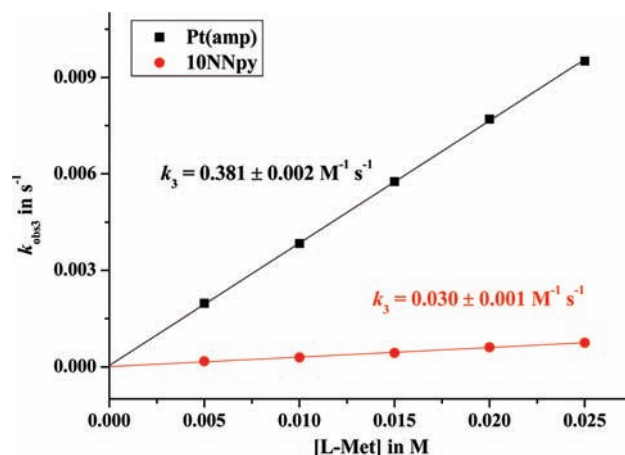


**Figure 6.** Plots of  $k_{\text{obs}3}$  vs L-methionine concentration for the reaction with 0.125 mM  $\text{Pt}(\text{amp})$  and 0.1 mM  $10\text{NNpy}$  at pH 7.4 and  $37 \text{ }^\circ\text{C}$  ( $I = 0.1 \text{ M}$  Hepes).

demanding coordination sphere of  $10\text{NNpy}$  and the larger entering nucleophile L-Met (compared to tu) may account for the 10 times slower displacement of water compared to the mononuclear complex. Furthermore, at pH 7.4, three hydroxo ligands are present in the coordination sphere of  $10\text{NNpy}$ , which leads to a significant decrease in electrophilicity of the Pt(II) center and therefore to slower reactions compared to  $\text{Pt}(\text{amp})$ , where only one hydroxo ligand is present. On the Pt(II) center where water is displaced, there is only one hydroxo ligand for both complexes. However, in the case of the dinuclear complex, the two metal centers interact with each other, and the one  $\text{Pt}(\text{OH})_2$  center of  $10\text{NNpy}$  also influences the other Pt(II) center. This interaction leads to a decrease in electrophilicity, since the leaving water ligand is coordinated *trans* to the bridging group.

No second reaction step was observed for both complexes. The obtained traces can be perfectly fitted to a single exponential. As mentioned before, the hydroxo ligand is strongly bound to the Pt(II) center and therefore cannot be displaced by L-Met. A change in the acidity of the hydroxo ligand following the

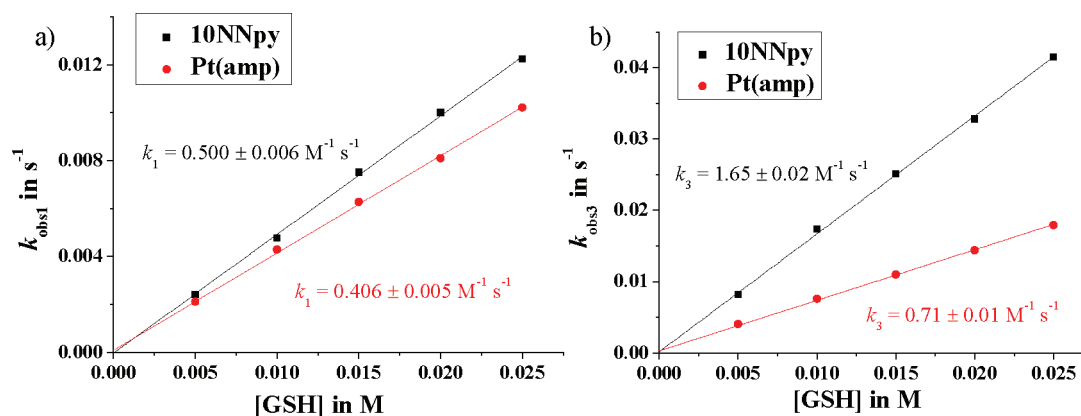


**Figure 7.** (a) Plots of  $k_{\text{obs}1}$  vs glutathione concentration for the reaction with 0.125 mM Pt(amp) and 0.1 mM 10NNpy at pH 2 and 25 °C ( $I = 0.01$  M, triflic acid). (b) Plots of  $k_{\text{obs}3}$  vs glutathione concentration for the reaction with 0.125 mM Pt(amp) and 0.1 mM 10NNpy at pH 7.4 and 37 °C ( $I = 0.1$  M, Heps).

coordination of L-Met is in principle possible. However, we suggest that the influence of L-Met on the electrophilicity of the metal center is too weak to convert the hydroxo ligand into a displaceable water molecule. Consequently, only one reaction occurs with L-Met at pH 7.4 and 37 °C for both complexes.

**Reactions with GSH.** The tripeptide glutathione (GSH,  $\gamma$ -L-glutamyl-L-cysteinyl-glycine) consists of the three amino acids glutamic acid, cysteine, and glycine. It is a ubiquitous thiol found in the cells of microorganisms, fungi, and plant and animal tissues, with intracellular concentrations between 0.1 and 10 mM.<sup>33</sup> GSH has numerous cellular functions, e.g., working as an antioxidant to protect cells against reactive oxygen species, UV radiation, and heavy metals such as mercury, cadmium, and lead.<sup>34,35</sup>

Furthermore, GSH is used in biological detoxification processes since it is known that complex formation between a heavy metal ion and GSH is the key step in detoxification.<sup>36–42</sup> The role of glutathione in the presence of cisplatin was studied in detail.<sup>43–45</sup> Glutathione is also present in significant concentrations in cytoplasm and may consequently react with platinum compounds before they can reach the DNA,<sup>46,47</sup> or may react with them after they are bound to DNA.<sup>47–49</sup> In a clinical phase-I study with cisplatin, it was observed that glutathione can be used as a so-called protecting agent since it interacts readily with the platinum drug and therefore reduces toxicity combined with less negative effects on the antitumor efficiency.<sup>50</sup> The role of glutathione appears to be dual, viz. it deactivates as well as activates cisplatin.<sup>51</sup> The higher activity of cisplatin has also been demonstrated by coadministering cisplatin and glutathione in patients. However, it is still not clear whether this increased activity arises from the reduced toxicity or from the modification of the platinum drug by binding to glutathione. Due to its significant biological role, the investigation of the reactivity of 10NNpy with GSH is of special interest.

Since it was clear that glutathione plays a crucial role in the reactions of platinum compounds with DNA, there has consequently been considerable interest in the reactions of glutathione with cisplatin and its analogues. For example, Odenheimer and Wolf reported that the reaction of cisplatin with 2 mol equivalents of glutathione resulted in a yellow solid that was meant to contain  $[\text{Pt}(\text{GS})_2]$ , where glutathione acts as a bidentate ligand and both the leaving groups and ammine ligands had been displaced.<sup>52</sup> Roos et al. also studied this reaction close to physiological conditions using UV–vis spectroscopy. They

found that an initial rapid reaction was followed by a much slower second reaction, but the UV–vis spectra did not allow identification of the generated products.<sup>53</sup> Reedjik et al. have shown that the diethylenetriamine complex  $[\text{Pt}(\text{dien})\text{Cl}]\text{Cl}$  reacts initially with glutathione to form a 1:1 complex with the ligand bound through sulfur, with a subsequent reaction to form a complex in which sulfur bridges between two Pt(dien) units.<sup>54</sup> Subsequently, Appleton et al. studied the reaction of the  $[\text{cis-Pt}(\text{NH}_3)_2(\text{OH}_2)_2]^{2+}$  cation with several S-containing amino acids and also with glutathione.<sup>55</sup> They also found a different reaction behavior with thiol-containing biomolecules, where the nucleophile could act as a bidentate as well as monodentate ligand. Sadler et al. investigated the reaction of  $[\text{Pt}(\text{en})\text{Cl}_2]$  (en = ethylenediamine) with glutathione and observed a bicyclic complex containing a 10-membered macrochelate ring.<sup>56</sup> Furthermore, polymeric structures via sulfur-bridged elements were found using NMR spectroscopy and mass spectrometry. Nowadays, it is well-known that the absorbance at 260 nm reflects the presence of platinum–sulfur and disulfide bonds, but the nature of the final reaction product remains unpredictable.<sup>57</sup>

On the basis of this information, we performed reactions of both complexes with glutathione, since Pt(amp) had so far not been investigated using GSH. First of all, reactions at pH 2 were investigated. We note that at pH 2, one of the major species is the zwitterionic form of GSH. The observed spectral changes during the reaction with GSH can be seen in Figure S15. Two reaction steps could be observed for both complexes at pH 2, one relatively rapid reaction that probably generated the 1:1 complex, followed by a drastically slower one. Plots of  $k_{\text{obs}1}$  against the glutathione concentration resulted in a linear dependence with no meaningful intercept for both complexes, and the experimental results obey eq 1 (Table 1 and also Table S5). The reactivities of the dinuclear and mononuclear complexes at pH 2 are nearly identical with rate constants  $k_1 = 0.500 \pm 0.006 \text{ M}^{-1} \text{ s}^{-1}$  for 10NNpy and  $k_1 = 0.406 \pm 0.005 \text{ M}^{-1} \text{ s}^{-1}$  for the Pt(amp) complex, as seen in Figure 7a (also Table 1). In terms of the lower nucleophilicity due to the lack of an electron donating methyl group at the sulfur atom, it is not surprising that the substitution reaction with GSH at pH 2 occurs slower compared to the reactions with L-Met and tu, where for all three nucleophiles coordination takes place through the sulfur donor. Consequently, the similar reactivity of the mono- and dinuclear complexes can again be explained by the weakness of



Scheme 3. Summary of Substitution Reactions of 10NNpy with Glutathione at Different pH Values

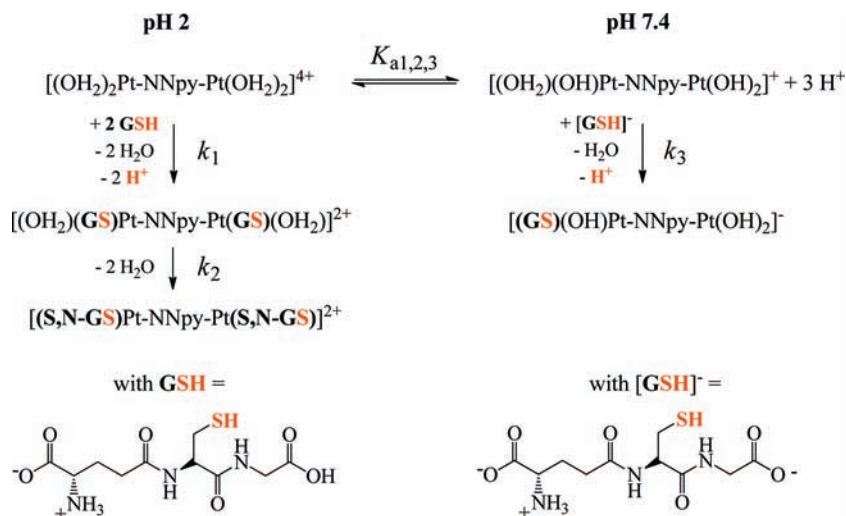


Table 2. Results of Mass Spectrometric Measurements for the Reaction of 10NNpy with Glutathione

<i>m/z</i>	charge	composition	intensity (24 h)	intensity (14 d)
542	+2	(C <sub>22</sub> H <sub>34</sub> N <sub>4</sub> Pt <sub>2</sub> )(C <sub>10</sub> H <sub>15</sub> N <sub>3</sub> O <sub>6</sub> S)	3.2%	33.6%
753	+2	(C <sub>22</sub> H <sub>34</sub> N <sub>4</sub> Pt <sub>2</sub> )(C <sub>10</sub> H <sub>16</sub> N <sub>3</sub> O <sub>6</sub> S) <sub>2</sub> (CF <sub>3</sub> SO <sub>3</sub> H)	1.7%	46.0%
828	+2	(C <sub>22</sub> H <sub>34</sub> N <sub>4</sub> Pt <sub>2</sub> )(C <sub>10</sub> H <sub>16</sub> N <sub>3</sub> O <sub>6</sub> S) <sub>2</sub> (CF <sub>3</sub> SO <sub>3</sub> H) <sub>2</sub>	3.7%	100%
914	+2	(C <sub>22</sub> H <sub>34</sub> N <sub>4</sub> Pt <sub>2</sub> )(C <sub>10</sub> H <sub>16</sub> N <sub>3</sub> O <sub>6</sub> S) <sub>2</sub> (CF <sub>3</sub> SO <sub>3</sub> H) <sub>2</sub> (CF <sub>3</sub> SO <sub>3</sub> )Na	1.6%	38.7%
927	+1	(C <sub>22</sub> H <sub>34</sub> N <sub>4</sub> Pt <sub>2</sub> )(CF <sub>3</sub> SO <sub>3</sub> )(OH) <sub>2</sub>	74.6%	4.7%
1059	+1	(C <sub>22</sub> H <sub>34</sub> N <sub>4</sub> Pt <sub>2</sub> )(CF <sub>3</sub> SO <sub>3</sub> ) <sub>2</sub> (OH)	100%	4.4%

the entering nucleophile as in the case of L-Met. Finally, we note that after binding to the Pt(II) center, the thiol group has to deprotonate since the hard and small proton cannot compete with the soft and large platinum metal. Consequently, the charge changes during the reaction from 4+ to 2+ (see Scheme 3).

The second reaction step is drastically slower than the first one for both complexes. We observed large spectral changes, and the solution turned yellow after a few hours, which was also observed by Appleton et al.<sup>55</sup> However, after three days the reaction still did not come to completion. Therefore, we repeated the kinetic measurements exclusively with the dinuclear 10NNpy complex at pH 2 and increased the temperature to 40 °C. Under these conditions, the reaction comes to an end after 40 h, and plots of  $k_{\text{obs}2}$  versus [GSH] show no dependence on the GSH concentration, as seen in Figure S16 (see also Table S6). The obtained  $k_{\text{obs}2}$  values obey eq 4 and result in a first-order rate constant  $k_2$  of  $(0.26 \pm 0.01) \times 10^{-4} \text{ s}^{-1}$ , as seen in Table 1.

As mentioned before, it is not easy to manifest the nature of the final product of this reaction. The independence of the nucleophile concentration suggests that glutathione could act as a bidentate ligand, and ring-closure could occur as a rate-determining step. However, these unusually large spectral changes could also be caused by the generation of sulfur bridged dimers and oligomers, which would then also result in no dependence on the GSH concentration. To enlighten these circumstances, we performed mass spectrometric measurements by reacting the 0.05 mM complex with 0.5 mM GSH at pH 2. Figure S17 shows a selected part of the recorded mass spectra within the interesting *m/z* range after a reaction time of 24 h and 14 days. It can be seen that the peaks of the free 10NNpy-aqua complex (*m/z* = 927 and *m/z* = 1059) nearly disappeared after the longer reaction time and that some complex-GSH product peaks increased in intensity. Table 2 summarizes the main

peaks, their corresponding composition, intensity (in % relative to the highest peak), and the charge of the species. The main reaction products include one platinum complex and two GSH molecules. After 14 days, no evidence for a higher substituted complex nor for oligomers with larger *m/z* values could be observed. From a combination of the kinetic observations and the mass spectrometric results, we suggest that one GSH ligand coordinated to each Pt(II) center, and in a second reaction step, ring-closure occurred, where GSH acts as a bidentate ligand and forms a five-membered S,N-chelate.<sup>55</sup>

Substitution reactions with GSH at pH 7.4 were also performed for both complexes, and the spectral changes observed during the reaction can be seen in Figure S18. The absorbance traces for both complexes again indicate a rapid first and a drastically slower second reaction. Plots of  $k_{\text{obs}3}$  versus glutathione concentration result in linear dependences for both complexes with no meaningful intercept, as shown in Figure 7b (see also Table S7), and can be analyzed using eq 3. In contrast to pH 2, 10NNpy reacts two times faster than Pt(amp), and both complexes show a higher reactivity at pH 7.4. Since we assumed that L-Met is the stronger nucleophile and should exhibit a faster water displacement, it is interesting to note that at pH 7.4 GSH shows the faster water displacement, and in the case of 10NNpy, even faster than thiourea (see Table 1).

At this point, it is necessary to take a closer look at the GSH species present in solution. The average  $\text{p}K_{\text{a}}$  values reported for the deprotonation of Glu-COOH, Gly-COOH, Cys-SH, and Glu-NH<sub>3</sub><sup>+</sup> are  $\text{p}K_{\text{a}1} = 2.06$ ,  $\text{p}K_{\text{a}2} = 3.50$ ,  $\text{p}K_{\text{a}3} = 8.69$ , and  $\text{p}K_{\text{a}4} = 9.62$ , respectively.<sup>58</sup> On the basis of the  $\text{p}K_{\text{a}}$  values, at pH 2 the zwitterion is one of the major species in solution and acts as an altogether neutral nucleophile (as in the case of L-Met), whereas at pH 7.4 the nucleophile is overall -1 negatively charged and therefore has a higher nucleophilicity. As a con-

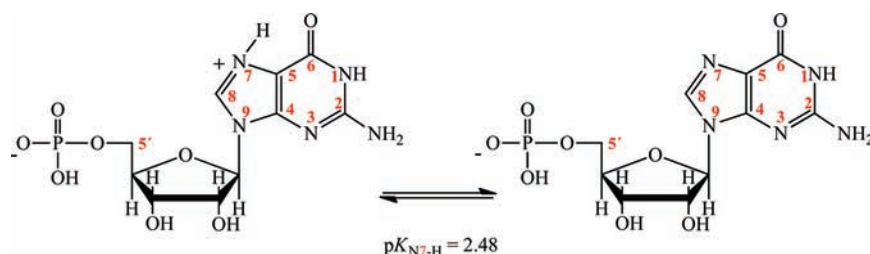


Figure 8. Structures of the acid–base equilibrium of guanosine-5'-monophosphate at pH 2.

sequence, water displacement by  $[\text{GSH}]^-$  can occur faster compared to GSH. For clarification, Scheme 3 summarizes the reactions of glutathione including structures for GSH and  $[\text{GSH}]^-$  at each pH value to show the changes in charge during the reaction. The **10NNpy** complex was used exclusively for illustration, but the reaction mechanism is also valid for its mononuclear analogue. This reaction behavior with negatively charged nucleophiles is of special importance when performing kinetic investigations as a function of pressure (see further discussion and activation parameters).

Besides the first reaction step, an extremely slow successive reaction was again observed for both complexes. Even at high temperatures (40 °C) and after 100 h, the reaction did not reach completion. Therefore, we did not investigate this reaction any further. The second-order rate constants  $k_1$  and  $k_3$  for the reaction at pH 2 and 7.4 are close to each other. To check whether the higher reactivity at pH 7.4 arises due to the higher temperature of 37 °C, we performed a concentration dependent study with **10NNpy** and GSH at pH 2 and 40 °C. The results are reported in Figure S19 and Table S8 and show a rate constant  $k_1$  of  $1.04 \pm 0.01 \text{ M}^{-1} \text{ s}^{-1}$  (Table 1), which is of course higher compared to the value at 25 °C, but significantly lower than for the reaction at pH 7.4. This means that the faster reaction with  $[\text{GSH}]^-$  is due to the different pH value and not due to the higher temperature.

**Reactions with 5'-GMP.** Guanosine-5'-monophosphate is a DNA model molecule and consists of a phosphate and sugar (2'-ribose) moiety connected to the nucleobase guanine (see Figure 1). It includes N-donor atoms and is a model for binding to a nucleobase. We performed substitution reactions at pH 2 and detected two successive reaction steps. The spectral changes during the reaction of **10NNpy** with 5'-GMP are very small. Due to the high absorbance of 5'-GMP, it was necessary to study the first reaction step with the platinum complex in excess. Thereby, plots of  $k_{\text{obs}1}$  versus platinum concentration and  $k_{\text{obs}2}$  versus nucleophile concentration both result in a linear dependence with no intercept (see Figure S20 and Table S9). The results imply that  $k_{\text{obs}}$  for the first and second substitution step can be expressed by eqs 1 and 2, where Nu = 5'-GMP, and the data are summarized in Table 1. At pH 2, the first reaction step of **10NNpy** ( $k_1 = 3.75 \pm 0.07 \text{ M}^{-1} \text{ s}^{-1}$ ) occurs more slowly compared to the first step of **Pt(amp)** ( $k_1 = 12.5 \pm 0.5 \text{ M}^{-1} \text{ s}^{-1}$ ),<sup>9</sup> whereas the second substitution step—the displacement of the last water ligand—is very similar for both complexes.

Keeping in mind the competition between N and S donors within the cell,<sup>58</sup> it is noted that 5'-GMP reacts faster than L-Met and GSH for both the mono- and dinuclear complexes under these experimental conditions (pH 2). Figure 8 depicts the structure of 5'-GMP at different pH's including atom numbering and  $pK_a$  values. It is known that the N7 site of 5'-GMP is strongly favored for binding to metal centers.<sup>59–64</sup> According to the  $pK_a(\text{N7})$  value of 2.48,<sup>61</sup> 65–75% of the 5'-GMP is protonated at N7 at pH 2, and therefore the molecule carries no charge,

whereas 25–35% of 5'-GMP has a negative charge due to a single deprotonated phosphate group. We assume that the non-protonated N7 of the negatively charged 5'-GMP reacts with the platinum center, and the acid–base equilibrium rapidly generates nonprotonated N7.<sup>9</sup> This is the reason for the faster reaction of 5'-GMP compared to L-Met and GSH. However, 5'-GMP as the N donor is not able to compete with thiourea under these conditions (see Table 1). In addition, mass spectrometric measurements were carried out to confirm the final product after the reaction. The main peaks in general confirm a 1:4 complex–nucleophile adduct where at each Pt(II) center the two water ligands have been displaced by two 5'-GMP ligands.

We also studied the substitution behavior under physiological conditions. Figure S21 shows the spectral changes observed during the reaction of **10NNpy** with 5'-GMP at pH 7.4. According to the  $pK_a$  values for the second phosphate oxygen ( $pK_a = 6.25$ ),<sup>57</sup> the nucleophile is partly 2-fold negatively charged at pH 7.4. Unfortunately, the absorbance changes during the reaction are too small and attempts to vary the complex and nucleophile concentrations were limited by the relatively high absorbance of free 5'-GMP and the low solubility of the complexes. Therefore, we did not study the reactions with the nucleophile 5'-GMP at pH 7.4 any further.

**Activation Parameters.** In addition, temperature and pressure dependence studies were performed to gain further insight into the nature of the substitution mechanism from the thermal and pressure activation parameters. Since all of the studied reactions did not include a back reaction, the thermal parameters  $\Delta H^\ddagger$  and  $\Delta S^\ddagger$  were determined by measuring the rate constants of the first and second reaction steps of each complex at a fixed nucleophile (tu, L-Met, GSH, and 5'-GMP) concentration as a function of the temperature (Tables S10–S15). Figure 9

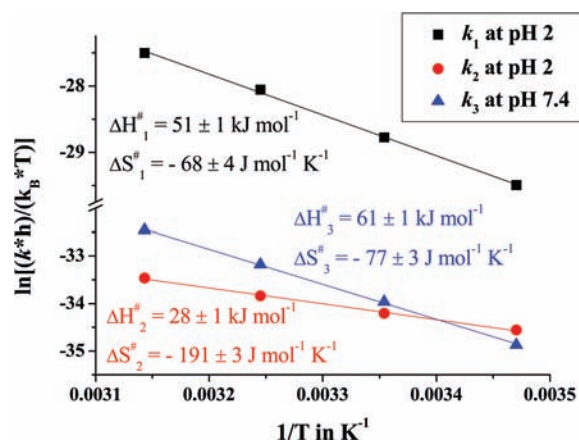


Figure 9. Eyring plots for the reaction of 0.1 mM **10NNpy** with 15 mM L-methionine at pH 2 ( $I = 0.01 \text{ M}$ , triflic acid) and pH 7.4 ( $I = 0.1 \text{ M}$ , Hepes).

Table 3. Activation Parameters for the Two Successive Reactions by a Range of Nucleophiles at pH 2

complex		$\Delta H_1^\ddagger$ [kJ mol <sup>-1</sup> ]	$\Delta S_1^\ddagger$ [J mol <sup>-1</sup> K <sup>-1</sup> ]	$\Delta V_1^\ddagger$ [cm <sup>3</sup> mol <sup>-1</sup> ]	$\Delta H_2^\ddagger$ [kJ mol <sup>-1</sup> ]	$\Delta S_2^\ddagger$ [J mol <sup>-1</sup> K <sup>-1</sup> ]	$\Delta V_2^\ddagger$ [cm <sup>3</sup> mol <sup>-1</sup> ]
10NNpy	tu	44 ± 2 <sup>4</sup>	-66 ± 6 <sup>4</sup>	-7.8 ± 0.1 <sup>4</sup>	37 ± 1 <sup>4</sup>	-128 ± 3 <sup>4</sup>	-12.6 ± 0.2 <sup>4</sup>
	L-Met	51 ± 1	-68 ± 4	-7.5 ± 0.2	28 ± 1	-191 ± 3	-20.2 ± 0.2
	GSH	57 ± 1	-59 ± 4	-7.5 ± 0.3			
	5'-GMP	51 ± 1	-66 ± 3				
Pt(amp)	tu	52 ± 3 <sup>9</sup>	-28 ± 9 <sup>9</sup>	-6.3 ± 0.1 <sup>9</sup>	35 ± 1 <sup>9</sup>	-95 ± 3 <sup>9</sup>	
	L-Met	52 ± 2 <sup>9</sup>	-72 ± 6 <sup>9</sup>	-12 ± 1 <sup>9</sup>	41 ± 5 <sup>9</sup>	-181 ± 16 <sup>9</sup>	-24 ± 4 <sup>9</sup>
	GSH	61 ± 1	-53 ± 3	-6.4 ± 0.2			
	5'-GMP	54 ± 2 <sup>9</sup>	-52 ± 8 <sup>9</sup>				

exemplarily shows the Eyring plots for the successive reactions of L-Met with 10NNpy at pH 2 and the single reaction step at pH 7.4. The Eyring plots for all other studied reactions at each pH are reported in Figures S22–S26. The activation parameters were calculated using the Eyring equation for which the observed first-order rate constants were converted to second-order rate constants ( $k = k_{\text{obs}}/[\text{Nu}]$ ), and the results are summarized in Tables 3 and 4 for measurements at pH 2 and 7.4, respectively. Pressure dependent studies were performed for the first step, and for some of the second substitution steps by measuring the rate constants  $k_{\text{obs}}$  for each complex at a fixed nucleophile concentration as a function of pressure (Figures S27–S31 and Tables S16–S20). The volumes of activation  $\Delta V^\ddagger$ , calculated from the slope of the plots of  $\ln(k_{\text{obs}})$  versus pressure, are summarized in Tables 3 (pH 2) and 4 (pH 7.4). By way of example, Figure 10 depicts plots of  $\ln(k_{\text{obs}})$  versus pressure for the successive reaction steps of 10NNpy with tu at different pH's. The  $k_{\text{obs}}$  values for all reactions increased with increasing pressure and show a linear dependence on pressure as depicted in Figure 10. The negative activation volumes are

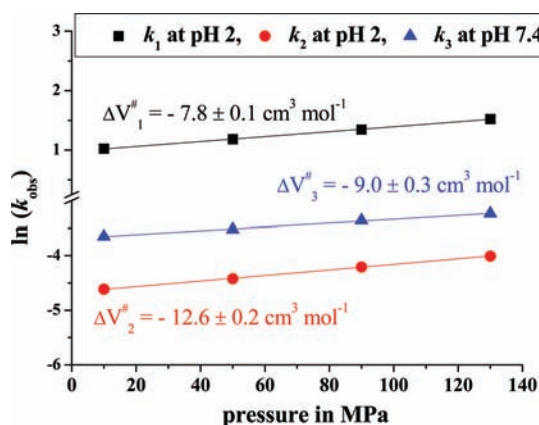


Figure 10. Plots of  $\ln(k_{\text{obs}})$  vs pressure for the reaction steps of 0.1 mM 10NNpy with 25 mM thiourea at 25 °C and pH 2 ( $I = 0.01$  M, triflic acid) and 37 °C and pH 7.4 ( $I = 0.1$  M, Hepes).

very typical for associative substitution reactions on square-planar complexes,<sup>65–67</sup> where the volume decrease results from bond formation on going from the square-planar reactant state to the trigonal bipyramidal transition state. This mechanistic assignment is furthermore in good agreement with the negative activation entropies found for the reaction steps for all nucleophiles studied (see Tables 3 and 4).

The trend in reactivity of the 10NNpy complex with the studied nucleophiles is also reflected in the activation enthalpy. The faster the reaction, the lower are the values for the activation enthalpy due to a more favored transition state, viz.,

Table 4. Activation Parameters for the Two Successive Reactions by a Range of Nucleophiles at pH 7.4

complex		$\Delta H_3^\ddagger$ [kJ mol <sup>-1</sup> ]	$\Delta S_3^\ddagger$ [J mol <sup>-1</sup> K <sup>-1</sup> ]	$\Delta V_3^\ddagger$ [cm <sup>3</sup> mol <sup>-1</sup> ]
10NNpy	tu	45 ± 1	-103 ± 4	-9.0 ± 0.3
	L-Met	61 ± 1	-77 ± 3	-13.3 ± 0.3
	GSH	66 ± 3	-33 ± 10	-2.6 ± 0.2
Pt(amp)	tu	43 ± 1	-102 ± 4	-5.2 ± 0.1
	L-Met	48 ± 1	-100 ± 4	-10.9 ± 0.7
	GSH	69 ± 2	-22 ± 6	-4.6 ± 0.1

tu < 5'-GMP < L-Met < GSH (at pH 2). The  $\Delta S_1^\ddagger$  values also become less negative in the order tu < 5'-GMP < L-Met < GSH (at pH 2). Moreover, the negative values for the activation entropy correlate with an associative substitution mechanism and can be interpreted in terms of a stronger associative character of the transition state due to stronger nucleophiles in the above-described order.

It is noted that the activation entropy as well as the activation volume for the second reaction step with L-Met, which is known to be a ring-closing reaction,<sup>9</sup> are significantly more negative compared to that for the first step. This can be explained by the ring closure itself, which implies deprotonation of the  $\text{NH}_3^+$  group. The released proton immediately undergoes strong solvation in solution and causes an increase in electrostriction which is accompanied by a volume collapse. Millero<sup>68</sup> reported the partial molar volume of a proton to be  $-4.2$  cm<sup>3</sup> mol<sup>-1</sup>. This volume collapse has to be added to the negative activation volume resulting from the chelation reaction and therefore results in such large negative activation volumes for both complexes, viz.  $\Delta V_2^\ddagger$  (10NNpy) =  $-20.2$  cm<sup>3</sup> mol<sup>-1</sup> and  $\Delta V_2^\ddagger$  (Pt(amp))<sup>9</sup> =  $-24$  cm<sup>3</sup> mol<sup>-1</sup>.

Furthermore, the substitution reaction with glutathione as the nucleophile is worth mentioning. GSH coordinates via the sulfur donor as mentioned before. During nucleophilic attack, the Pt(II) center competes with the hydrogen atom of the thiol donor, although the small and hard proton cannot compete with the large and soft platinum center. As a consequence, the proton is released during the reaction. GSH is not comparable with L-Met, because the proton liberation in the case of L-Met is necessary before nucleophilic attack can occur, whereas in the case of GSH the deprotonation occurs after the nucleophilic attack. This is important since it explains why we observe relatively negative activation volumes due to proton liberation for L-Met, but not for GSH (see Tables 3 and 4).

A closer look has to be taken at the activation volumes for the reaction with GSH at pH 7.4. As mentioned above (see Scheme 3), glutathione at pH 7.4 exists predominantly as a  $-1$  charged nucleophile, and substitution of the water ligand results in a decrease in charge from  $+1$  to  $-1$  for both the di- and mononuclear complexes. The activation volumes for this

reaction are  $\Delta V_3^\ddagger = -2.6 \pm 0.2 \text{ cm}^3 \text{ mol}^{-1}$  (**10NNpy**) and  $\Delta V_3^\ddagger = -4.6 \pm 0.1 \text{ cm}^3 \text{ mol}^{-1}$  (**Pt(amp)**), and these activation volumes have the smallest absolute values observed for all studied reactions. The value of  $\Delta V^\ddagger$  is composed of the contribution for bond formation, which is expected to be significantly negative for an associative mechanism, and the contribution of charge neutralization, which leads to an enlarged solvation shell on forming the transition state and consequently to a less negative activation volume.

**Cytostatic Activity.** Dr. Thomas Huhn from the University of Konstanz and his team performed cell tests on the previously<sup>4</sup> synthesized dinuclear **NNpy** complex system. They examined the cytotoxicity of the tetra-chloro complexes and the ligands using the AlamarBlue assay in the human cervix carcinoma cell line HeLa S3. Fluorescence measurements and comparison with a negative control gave the relative number of cells that survived the treatment. The results revealed that only complex **2** is cytostatically active, i.e., the here studied **10NNpy** complex. We found a rather good  $IC_{50}$  value of  $6.0 \pm 0.8 \mu\text{M}$  for complex **2**, which describes the concentration at which 50% of the cells remained viable with respect to the control. The resulting dose–response curve for the HeLa S3 cell line is shown in Figure S32, and the experimental results are summarized in Table S21. Cisplatin was also tested as a reference compound and exhibited an  $IC_{50}$  value of  $1.2 \pm 0.4 \mu\text{M}$ . We note that the free ligand itself shows some cytotoxic activity ( $36 \mu\text{M}$ , not shown), but the  $IC_{50}$  values clearly demonstrated that complex **2** results in a much higher activity than the ligand. The chloro complexes were used for the cell tests instead of the corresponding aqua species due to their biological and medical relevance.

The **10NNpy** complex is a dinuclear species, and it is known from the literature that polynuclear complexes form different DNA adducts due to their ability to form long-ranged inter-strand cross-links.<sup>70</sup> Widespread studies in cell-free systems indicate that the formation of interstrand cross-links is a major event for di- or polynuclear complexes.<sup>71</sup> Thus, dinuclear cytostatically active complexes may have the advantage of unique DNA adduct formation.<sup>72</sup> As a consequence, the caused DNA damage cannot be sufficiently repaired, and polynuclear complexes may help in terms of overcoming Pt-drug resistance.

Finally, we want to turn to the different isomers of **10NNpy**, their role as cytostatically active complexes, and the kinetic investigations. It is known from the literature that the cytostatic activity can depend on the presence of NH groups in the carrier ligand due to possible guanine–O6–NH<sup>73–76</sup> and/or phosphate–NH<sup>75–82</sup> intramolecular hydrogen bonding. Consequently, different isomers influence these possible interactions, and as a result different configurations of DNA adducts occur. Therefore, different configurations can cause different cytostatic activities. In our case, the achiral *N,N*-ligand obtains a stereogenic N-center after coordination to the metal. We assume that the chirality of the **10NNpy** isomers has no significant influence on the reaction rates, because the acidic N-bound proton is sterically nondemanding and, as demonstrated previously, shows a rapid H-exchange.<sup>4</sup> In other words, the different isomers of **10NNpy** are structurally almost equal to each other. Furthermore, the nucleophilic attack occurs above or below the square planar coordination sphere, and one can hardly expect that the position of the small proton significantly influences the nucleophilic attack. Moreover, it is noted that the **10NNpy**–chloro complex shows cytostatic activity, although a mixture of isomers is present in solution. The fact that the

configuration at the NHR<sub>2</sub> donor cannot be fixed due to rapid H-exchange implicates that the nature of the active isomer cannot be determined. Maybe the mixture itself is cytostatically active due to the strong similarity of the isomers.

## CONCLUSION

In this study, we focused on two known complexes previously studied in our group, viz. a dinuclear Pt(II) complex with a bidentate pyridine unit linked to a secondary amine, where the two metal centers are connected by an aliphatic chain of 10 methylene groups (**10NNpy**),<sup>4</sup> and its mononuclear analogue (**Pt(amp)**)<sup>9</sup> without a bridging element. We wanted to gain more insight into the reactivity of these *N,N*-containing complexes under physiological conditions with biologically relevant nucleophiles, viz. thiourea, *L*-methionine, reduced glutathione, and guanosine 5'-monophosphate. First, the reactivity of both complexes with the selected nucleophiles was investigated at pH 2, where both complexes exist exclusively in their aqua form. The substitution of coordinated water by the selected nucleophiles was studied under pseudo-first-order conditions as a function of nucleophile concentration, temperature, and pressure, using stopped-flow techniques and UV–vis spectroscopy. The reactivity of the aqua complexes **10NNpy** and **Pt(amp)** was found to be in the order  $tu \gg 5'\text{-GMP} > L\text{-Met} > \text{GSH}$  at pH 2. Thiourea is the strongest nucleophile and exhibits by far the fastest substitution reactions for both complexes. This strong interaction between platinum and S-donor nucleophiles is also of interest in terms of their chemoprotective ability. Especially against nephrotoxicity, thiourea or methionine was used to suppress the coordination of platinum to S-donor proteins, which is responsible for several side effects.<sup>7,10</sup> Furthermore, the N-donor nucleophile guanosine 5'-monophosphate is able to compete with the S-donor nucleophiles *L*-Met and GSH at pH 2. These observations are of special interest, since under biological conditions and within the cell, these S-donor biomolecules are present in relatively high concentrations and therefore compete with the ultimate target of the platinum drug, viz. the DNA.<sup>31,32</sup> Moreover, we observed ring-closure reactions for the dinuclear **10NNpy** complex with *L*-Met and GSH, which confirms our assumption of a rather good stability of the dinuclear system, because the amine linker is not substituted by a second *trans* labilizing S-donor nucleophile.

In a next step, the reactions with **10NNpy** and **Pt(amp)** were studied at a higher pH (7.4) and higher temperature (37 °C) to mimic the physiological conditions by using the same selected nucleophiles. At a higher pH, the aqua complexes undergo stepwise deprotonation. The reactive species of **Pt(amp)** at pH 7.4 was found to be the aqua–hydroxo complex (15%), and the aqua–trihydroxo complex (56%) in the case of **10NNpy**. In general, the observed rate constants are lower compared to those at pH 2. This is ascribed to the less labile and less electrophilic Pt(II) centers due to the coordination of hydroxo ligands. The reactivity at pH 7.4 for **10NNpy** with the selected nucleophiles was found to be  $\text{GSH} > tu > L\text{-Met}$ , and for **Pt(amp)**,  $tu > \text{GSH} > L\text{-Met}$ . This difference in reactivity at pH 7.4 arises from the different species distribution due the different  $pK_a$  values of the mono- and dinuclear complexes. The **10NNpy** complex exists at 56% in its reactive form compared to only 15% for **Pt(amp)**. The spectral changes observed during the reaction with 5'-GMP at pH 7.4 were too small to perform kinetic concentration-dependent studies. It is noted that the order of reactivity is different at pH 7.4 compared to pH 2.

Glutathione reacts faster, which can be explained in terms of the acidity of its functional groups. At pH 2, GSH exists predominantly in its zwitterionic form, whereas at pH 7.4 it acts as a  $-1$  charged nucleophile and therefore exhibits a higher nucleophilicity.

The acceleration of the reactions by pressure points to an associative substitution mechanism, which is also supported by the significantly negative activation entropies typical for square planar Pt(II) complexes. It is obvious that  $\Delta S^\ddagger_2$  and  $\Delta V^\ddagger_2$  for the second substitution step with L-methionine also exhibits such negative values. The reaction involves a ring-closure process, which initially requires  $\text{NH}_3^+$  deprotonation prior to nucleophilic attack. This proton liberation causes a volume collapse due to highly condensed charge creation in an aqueous medium, which adds to the volume collapse resulting from bond formation (ring-closure) and therefore leads to such significantly negative values.

## ■ ASSOCIATED CONTENT

### ■ Supporting Information

Mass spectrometric and NMR measurements; UV-vis spectra; pH dependence; distribution diagrams; and concentration, temperature, and pressure dependent studies for all reactions studied. The tables summarize all data for all reactions at different concentrations, temperatures, and pressures, and the results of the cell tests. This material is available free of charge via the Internet at <http://pubs.acs.org>.

## ■ AUTHOR INFORMATION

### Corresponding Author

\*E-mail: [vaneldik@chemie.uni-erlangen.de](mailto:vaneldik@chemie.uni-erlangen.de).

### Notes

The authors declare no competing financial interest.

## ■ ACKNOWLEDGMENTS

The authors gratefully acknowledge continued financial support from the Deutsche Forschungsgemeinschaft. The authors kindly thank Malin Bein for help with the biological assays and Dr. Thomas Huhn for the kind cooperation. They also thank Prof. Dr. Ivana Ivanović-Burmazović and Oliver Tröppner for their support with the mass spectrometric measurements.

## ■ REFERENCES

- (1) Werb, Z. *Nature Medicine* **2010**, *16*, 1071.
- (2) (a) Scherer, W. F.; Syverton, J. T.; Gey, G. O. *J. Exp. Med.* **1953**, *97*, 695–710. (b) Swanson, P. E.; Carroll, S. B.; Zhang, X. F.; Mackey, M. A. *Am. J. Pathol.* **1995**, *146*, 963–971. (c) Kampinga, H. H.; Hiemstra, Y. S.; Konings, A. W. T.; Dikomey, E. *Int. J. Radiat. Biol.* **1997**, *72*, 293–301. (d) Whitfield, M. L.; Sherlock, G.; Saldanha, A. J.; Murray, J. I.; Ball, C. A.; Alexander, K. E.; Matese, J. C.; Perou, C. M.; Hurt, M. M.; Brown, P. O.; Botstein, D. *Mol. Biol. Cell* **2002**, *13*, 1977–2000. (e) Eger, S.; Immel, T. A.; Claffey, J.; Müller-Bunz, H.; Tacke, M.; Groth, U.; Huhn, T. *Inorg. Chem.* **2010**, *49*, 1292–1294.
- (3) Rosenberg, B.; VanCamp, L.; Trosko, J. E.; Mansour, V. H. *Nature* **1969**, *222*, 385–386.
- (4) Hochreuther, S.; Puchta, R.; van Eldik, R. *Inorg. Chem.* **2011**, *50*, 8984–8996.
- (5) (a) Jakupec, M. A.; Galanski, M.; Keppler, B. K. *Rev. Physiol. Biochem. Pharmacol.* **2003**, *146*, 1–54. (b) van Rijt, S. H.; Sadler, P. J. *Drug Discovery Today* **2009**, *14*, 1089–1097. (c) Lovejoy, K. S.; Lippard, S. J. *Dalton Trans.* **2009**, *48*, 1065–1069.
- (6) Reedijk, J. *Chem. Rev.* **1999**, *99*, 2499–2510.
- (7) Reedijk, J. *Chem. Commun.* **1996**, 801–806.
- (8) Reedijk, J. *Inorg. Chim. Acta* **1992**, *873*, 198–200.
- (9) Summa, N.; Schiessl, W.; Puchta, R.; van Eikema Hommes, N.; van Eldik, R. *Inorg. Chem.* **2006**, *45*, 2948–2959.
- (10) Burchenal, J. H.; Kalaher, K.; Dew, K.; Lokys, L.; Gale, G. *Biochimie* **1978**, *60*, 961–965.
- (11) Hureau, C.; Blondin, G.; Charlot, M.-F.; Philouze, C.; Nierlich, M.; Cesario, M.; Anxolabehere-Mallart, E. *Inorg. Chem.* **2005**, *44*, 3669–3683.
- (12) Hofmann, A.; van Eldik, R. *Dalton Trans.* **2003**, 2979–2985.
- (13) Hamid, R.; Rotshteyn, Y.; Rabadi, L.; Parikh, R.; Bullock, P. *Toxicol. In Vitro* **2004**, *18*, 703–710.
- (14) van Eldik, R.; Gaede, W.; Wieland, S.; Kraft, J.; Spitzer, M.; Palmer, D. A. *Rev. Sci. Instrum.* **1993**, *64*, 1355–1357.
- (15) Spitzer, M.; Gartig, F.; van Eldik, R. *Rev. Sci. Instrum.* **1988**, *59*, 2092.
- (16) (a) Appleton, T. G.; Berry, R. D.; Davis, C. A.; Hall, J. R.; Kimlin, H. A. *Inorg. Chem.* **1984**, *23*, 3514–3521. (b) Boreham, C. J.; Broomhead, J. A.; Fairlie, D. P. *Aust. J. Chem.* **1981**, *34*, 659–664.
- (17) (a) Faggiani, R.; Lippert, B.; Lock, C. J. L.; Rosenberg, B. *Inorg. Chem.* **1978**, *17*, 1941–1945. (b) Qu, Y.; Farrell, N. *J. Inorg. Biochem.* **1990**, *40*, 255–264.
- (18) Brière, K. M.; Goel, R.; Shirazi, F. H.; Stewart, D. J.; Smith, I. C. P. *Cancer Chemother. Pharmacol.* **1996**, *37*, 518–524.
- (19) Prenzler, P. D.; McFadyen, W. D. *J. Inorg. Biochem.* **1997**, *68*, 279–282.
- (20) Ashby, M. T. *Comments Inorg. Chem.* **1990**, *10*, 297–313.
- (21) Murray, S. G.; Hartley, F. R. *Chem. Rev.* **1981**, *81*, 365–414.
- (22) Mahal, G.; van Eldik, R. *Inorg. Chem.* **1985**, *24*, 4165–4170.
- (23) Mahal, G.; van Eldik, R. *Inorg. Chim. Acta* **1987**, *127*, 203–208.
- (24) Hofmann, A.; Jaganyi, D.; Munro, O. Q.; Liehr, G.; van Eldik, R. *Inorg. Chem.* **2003**, *42*, 1688–1700.
- (25) Lide, D. R. *Handbook of Chemistry and Physics*; CRC Press: New York, 1995.
- (26) Cohn, E. J.; Edsall, J. T. *Proteins, Amino Acids and Peptides as Ions and Dipolar Ions*; Reinhold Publishing Corporation: New York, 1943.
- (27) Hofmann, A.; Dahlenburg, L.; van Eldik, R. *Inorg. Chem.* **2003**, *42*, 6528–6538.
- (28) Appleton, T. G.; Connor, J. W.; Hall, J. R. *Inorg. Chem.* **1988**, *27*, 130–137.
- (29) Barnham, K. J.; Djuran, M. I.; Del Socorro Murdoch, P.; Ranford, J. D.; Sadler, P. J. *Inorg. Chem.* **1996**, *35*, 1065–1072.
- (30) Summa, N.; Maigut, J.; Puchta, R.; van Eldik, R. *Inorg. Chem.* **2007**, *46*, 2094–2104.
- (31) Oehlsen, M. E.; Qu, Y.; Farrell, N. *Inorg. Chem.* **2003**, *42*, 5498–5506.
- (32) Oehlsen, M. E.; Hegmans, A.; Qu, Y.; Farrell, N. *J. Biol. Inorg. Chem.* **2005**, *10*, 433–442.
- (33) (a) Meister, A. *J. Biol. Chem.* **1988**, *263*, 17205–17208. (b) Meister, A.; Anderson, M. E. *Annu. Rev. Biochem.* **1983**, *52*, 711–760.
- (34) Pompella, A.; Visvikis, A.; Paolicchi, A.; De Tata, V.; Casini, A. F. *Biochem. Pharmacol.* **2003**, *66*, 1499–1503.
- (35) Meister, A.; Tate, S. S. *Annu. Rev. Biochem.* **1976**, *45*, 559–604.
- (36) Chu, G. *Biol. Chem.* **1994**, *269*, 787–790.
- (37) Fauchon, M.; Lagniel, G.; Aude, J.-C.; Lombardia, L.; Soularue, P.; Petat, C.; Marguerie, G.; Sentenac, A.; Werner, M.; Labarre, J. *Mol. Cell* **2002**, *9*, 713–723.
- (38) Jamieson, D. *Nat. Genet.* **2002**, *31*, 228–230.
- (39) Li, Z.-S.; Lu, Y.-P.; Zhen, R.-G.; Szczycka, M.; Thiele, D. J.; Rea, P. A. *Proc. Natl. Acad. Sci. U.S.A.* **1997**, *94*, 42–47.
- (40) Li, Z.-S.; Szczycka, M.; Lu, Y.-P.; Thiele, D. J.; Rea, P. A. *J. Biol. Chem.* **1996**, *271*, 6509–6517.
- (41) Singhal, R. K.; Anderson, M. E.; Meister, A. *FASEB J.* **1987**, *1*, 220–223.
- (42) Vido, K.; Spector, D.; Langniel, G.; Lopez, S.; Toledano, M. B.; Labarre, J. *J. Biol. Chem.* **2001**, *276*, 8469–8474.
- (43) Pratesi, G.; DalBo, L.; Poalicchi, A.; Tonarelli, P.; Tongiani, R.; Zunino, F. *Ann. Oncol.* **1995**, *6*, 283–289.

- (44) Sastre, J.; Diazrubio, E.; Blanco, J.; Cifuentes, L. *Oncol. Rep.* **1996**, *3*, 1149–1152.
- (45) Bernstein, E. F.; Pass, H. A.; Glass, J.; Deluca, A. M.; Cook, S.; Fisher, J.; Cook, J. A. *Int. J. Oncol.* **1995**, *7*, 353–358.
- (46) Kulamowicz, I.; Olinski, R.; Walter, Z. *Z. Naturforsch.* **1984**, *39C*, 184–190.
- (47) Eastman, A. *Chem. Biol. Interact.* **1987**, *61*, 241–248.
- (48) Eastman, A.; Barry, M. A. *Biochemistry* **1987**, *26*, 3303–3307.
- (49) Micetich, K.; Zwelling, L. A.; Kohn, K. W. *Cancer Res.* **1983**, *43*, 3609–3613.
- (50) Smith, J. F.; Bowman, A.; Perren, T.; Wilkinson, P.; Presciotti, R. J.; Quinn, K. J.; Tedeschi, M. *Ann. Oncol.* **1997**, *8*, 569–574.
- (51) Valckova, E.; Dudones, L. P.; Bose, R. N. *Pharm. Res.* **2002**, *19*, 124.
- (52) Odenheimer, B.; Wolf, W. *Inorg. Chim. Acta* **1982**, *36*, 1955–1964.
- (53) Roos, I. A. G.; Stokes, K. H. *Abstracts of Papers, Third International Conference on the Chemistry of the platinum Group metals, Sheffield, U.K., July 1987*; Royal Society of Chemistry: London, 1987; Abstract O-36.
- (54) Lempers, E. L. M.; Inagaki, K.; Reedijk, J. *Inorg. Chim. Acta* **1988**, *152*, 201–207.
- (55) Appleton, T. G.; Connor, J. W.; Hall, J. R.; Prenzler, P. D. *Inorg. Chem.* **1989**, *28*, 2030–2037.
- (56) Del Socorro Murdoch, P.; Kratochwil, N. A.; Parkinson, J. A.; Patriarca, M.; Sadler, P. J. *Angew. Chem.* **1999**, *38*, 2949–2951.
- (57) Suchánková, T.; Vojtíšková, M.; Reedijk, J.; Brabec, V.; Kašpárková, J. *J. Biol. Inorg. Chem.* **2009**, *14*, 75–87.
- (58) Oram, P. D.; Fang, X.; Fernando, Q.; Letkeman, D. *Chem. Res. Toxicol.* **1996**, *9*, 709–712.
- (59) Lippert, B. *Cisplatin: Chemistry and Biochemistry of a Leading Anticancer Drug*; Wiley-VCH: Zürich, Switzerland, 1999; pp 183–221.
- (60) Arpalahiti, J.; Lehtikoinen, P. *Inorg. Chem.* **1990**, *29*, 2564–2567.
- (61) Zhu, S.; Matilla, A.; Tercero, J. M.; Vijayaragavan, V.; Walmsley, J. A. *Inorg. Chim. Acta* **2004**, *357*, 411–420.
- (62) Arpalahiti, J.; Lippert, B. *Inorg. Chem.* **1990**, *29*, 104–110.
- (63) Bugarčić, Z. D.; Heinemann, F. W.; van Eldik, R. *Dalton Trans.* **2004**, *2*, 279–286.
- (64) Martin, R. B. *Acc. Chem. Res.* **1985**, *18*, 32–38.
- (65) Stochel, G.; van Eldik, R. *Coord. Chem. Rev.* **1999**, *187*, 329–374.
- (66) Helm, L.; Elding, L. I.; Merbach, A. E. *Helv. Chim. Acta* **1984**, *67*, 1453–1460.
- (67) Helm, L.; Elding, L. I.; Merbach, A. E. *Helv. Chim. Acta* **1985**, *24*, 1719–1721.
- (68) (a) Millero, F. J. *Water and Aqueous Solutions: Structure, Thermodynamics and Transport Properties*; Wiley-Interscience: New York, 1972; Chapter 13, p 532. (b) Millero, F. J. *Chem. Rev.* **1971**, *71*, 163–169.
- (69) Berners-Price, S. J.; Appleton, T. G. *Platinum-based Drugs in Cancer Therapy*; Kelland, L. R., Farrell, N. P., Eds.; Humana Press Inc.: Totowa, NJ, 2000.
- (70) (a) Cox, J. W.; Berners-Price, S. J.; Davies, M. S.; Qu, Y.; Farrell, N. *J. Am. Chem. Soc.* **2001**, *123*, 1316–1326. (b) Brabec, V.; Kasparova, J. *Drug Resist. Updates* **2005**, *8*, 131–146.
- (71) Brabec, V.; Kašpárková, J.; Vrána, O.; Nováková, O.; Cox, J. W.; Qu, Y.; Farrell, N. *Biochemistry* **1999**, *38*, 6781–6790.
- (72) (a) Kloster, M. B. G.; Hannis, J. C.; Mudiman, D. C.; Farrell, N. *Biochemistry* **1999**, *38*, 14731–14737. (b) Kašpárková, J.; Zehnulova, J.; Farrell, N.; Brabec, V. *J. Biol. Chem.* **2002**, *277*, 48076–48086. (c) Hegmans, A.; Berners-Price, S. J.; Davies, M. S.; Thomas, D. S.; Humphreys, A. S.; Farrell, N. *J. Am. Chem. Soc.* **2004**, *126*, 2166–2180. (d) Qu, Y.; Tran, M.-C.; Farrell, N. P. *J. Biol. Inorg. Chem.* **2009**, *14*, 969–977.
- (73) Sherman, S. E.; Gibson, D.; Wang, A. H. J.; Lippard, S. J. *J. Am. Chem. Soc.* **1988**, *110*, 7368–7381.
- (74) Xu, J.; Natile, G.; Intini, F. B.; Marzilli, L. G. *J. Am. Chem. Soc.* **1990**, *112*, 8177–8179.
- (75) Kiser, D.; Intini, F. P.; Xu, Y.; Natile, G.; Marzilli, L. G. *Inorg. Chem.* **1994**, *33*, 4149–4158.
- (76) Guo, Z.; Sadler, P. J.; Zang, E. *Chem. Commun.* **1997**, *1*, 27–28.
- (77) Berners-Price, S. J.; Frey, U.; Ranford, J. D.; Sadler, P. J. *J. Am. Chem. Soc.* **1993**, *115*, 8649–8659.
- (78) Berners-Price, S. J.; Ranford, J. D.; Sadler, P. J. *Inorg. Chem.* **1994**, *33*, 5842–5846.
- (79) Berners-Price, S. J.; Frenkiel, T. A.; Ranford, J. D.; Sadler, P. J. *J. Chem. Soc., Dalton Trans.* **1992**, 2137–2139.
- (80) Bloemink, M. J.; Heetebrij, R. J.; Inagaki, K.; Kidani, Y.; Reedijk, J. *Inorg. Chem.* **1992**, *31*, 4656–4661.
- (81) Reedijk, J. *Inorg. Chim. Acta* **1992**, 198–200, 873–881.
- (82) Fouts, C. S.; Marzilli, L. B.; Byrd, R. A.; Summers, M. F.; Zon, G.; Shinozuka, K. *Inorg. Chem.* **1988**, *27*, 366–376.